engineering proceedings

MDPI

Proceeding Paper

Multi-Constellation/Multi-Frequency GNSS Signal Degradation Due to Foliage and Reflective Environments †

Uttama Dutta [1,2,*] and Jan Johansson [1,2]

[1] Department of Space, Earth and Environment, Chalmers University of Technology, 412 96 Gothenburg, Sweden; jan.johansson@chalmers.se
[2] Department of Measurement Science and Technology, RISE Research Institutes of Sweden, Brinellgatan 4, 504 62 Borås, Sweden
* Correspondence: uttama.dutta@ri.se
† Presented at the European Navigation Conference 2023, Noordwijk, The Netherlands, 31 May–2 June 2023.

Abstract: Present day GNSS offers a variety of signals from different satellite constellations and at various frequencies. This paper is based on the work conducted in the project SiL 2.0 and will focus on the study of multi-constellation/multi-frequency GNSS signals as received on top of construction equipment as part of the SiL 2.0 dissemination solution. This paper aims to study the impact of foliage and reflective environments on the various signals of multi-constellation GNSS with a focus on GPS and Galileo. Signal strength indicators (SSI) have been used as a measure to understand the shadowing environment around a stationary GNSS antenna mounted on an excavator. It is quite clear from the analysis that traditional GPS L2 signals, C2W and L2W, are weaker in strength than the L2C and L1 C/A signals, and this is found to be consistent for all of the GPS satellites. The effect of signal degradation due to bending over sharp metallic edges is also discussed.

Keywords: GNSS; multi-constellation; signal bending or diffraction; reflective environment; foliage signal degradation

check for updates

Citation: Dutta, U.; Johansson, J. Multi-Constellation/Multi-Frequency GNSS Signal Degradation Due to Foliage and Reflective Environments. *Eng. Proc.* **2023**, *54*, 2. https://doi.org/10.3390/ENC2023-15454

Academic Editors: Tom Willems and Okko Bleeker

Published: 29 October 2023

Copyright: © 2023 by the authors. Licensee MDPI, Basel, Switzerland. This article is an open access article distributed under the terms and conditions of the Creative Commons Attribution (CC BY) license (https://creativecommons.org/licenses/by/4.0/).

1. Introduction

Multi-constellation GNSS now offers a wide range of services, signals and frequencies to choose from. The L1 C/A signal remains the leading signal of the well-established GPS and is used in almost all GPS devices and technology. L2C, the new civilian-use GPS signal, is used to improve the accuracy of navigation, offers a signal that is very easy to track and provides signal redundancy for adverse situations. The improvement brought about by using L2C in GPS-based ionospheric research and monitoring has already been explored elsewhere [1,2]. In this study, we try to compare the positioning performance of L2C with traditional GPS signals and show that these signals have improved reliability in comparison to the traditional ones for field applications such as that on an excavator.

Andrei et al. [3,4] analysed the performance of Galileo L10 (tenth launch) in terms of Signals-in-Space (SiS) availability and accuracy and concluded with their numerical results that these satellites comply with their target values in terms of SiS performance. This demonstrates the reliability, robustness and consistency of the signal transmission for Galileo and is probably due to (apart from other technical improvements) the use of highly stable Passive Hydrogen Masers on board the satellites [5]. In this study, we also try to study Galileo signal positioning performance using signals transmitted on the E1 and E5b frequencies. This paper is based on the work conducted in the project SiL 2.0 and will focus on the study of multi-constellation/multi-frequency GNSS signals as received on top of construction equipment as part of the SiL 2.0 dissemination solution.

Section 2 briefly talks about the SiL 2.0 project; Section 3 gives the details of the data collection with the excavator. Section 4 shows the results. Section 4.1 deals with signal degradation due to foliage and compares different GNSS signals on the basis of degradation

of their signal strength indicators. Section 4.2 deals with signal degradation due to reflective environments and discusses how a metallic edge could bring about such a degradation. Section 5 gives the conclusions.

2. SiL 2.0 Project

'Stomnät i Luften' 2.0 (SiL 2.0) is a research and innovation project with the overall goal to prepare the Swedish Transport Administration's construction operations for the challenges of the future regarding geodesy and machine control. This 3-year project financed by the Swedish Transport Administration uses GNSS-RTK position determination with the so-called project-adapted network RTK (PaNRTK) technology, which is used for geodetic measurements, machine control, etc., in large construction projects. In this study, a GNSS receiver mounted on the top of an excavator is used to study the positioning performance using GNSS PPP in an environment with foliage and reflective surfaces. The results from GipsyX version 2.3 [6,7] using PPP corrections as well as raw RINEX data are discussed.

3. Data Collection with the Excavator

Data collected during 3–11 September 2022 from a Septentrio PolarRx5 GNSS receiver, with its antenna (Leica AS10) mounted on an excavator, was used to study GNSS performance. The experimental set up demonstrating the antenna environment is as shown in Figure 1 below. From Figure 1c, it is clear that the antenna mounted on top of the excavator would experience signal degradation not only due to the metallic walls of the excavator but also from the building on the left (located at a distance of around 7 m), the hillock on the front and also from the vegetation on the right (located at a distance of around 10 m). It is to be noted for Figure 1c that the excavator is facing the NW direction, which means that the tree is located roughly on the NW side and the house on the SE direction.

(**a**)

Figure 1. *Cont.*

(**b**) (**c**)

Figure 1. The experimental set up. (**a**) The GNSS antenna marked with a green circle on top of the excavator. (**b**) Top view of the excavator showing the GNSS antenna. (**c**) The excavator facing NW direction with the tree on the right and the house on the left.

4. Results

4.1. Signal Degradation Due to Foliage

In the following discussions, RINEX 3 data collected from the GNSS receiver on the excavator during 12:00 h on 3 September 2022 to around 10:00 h on 5 September 2022 were used for analysis. During this period, the excavator was stationary, and therefore, this is referred to as the 'stationary period' in multiple places in the document. The excavator at the beginning of the experiment on 3 September is made to face north, as mentioned before. Figure 2 shows the GNSS satellite visibility. During 40 percent of this time duration, 11 GPS satellites were visible, and 8 Galileo satellites were visible 50% of the time. A minimum of 5–7 satellites/constellations (GPS, Galileo and Glonass) and 22 satellites in total were visible almost all of the time during this period.

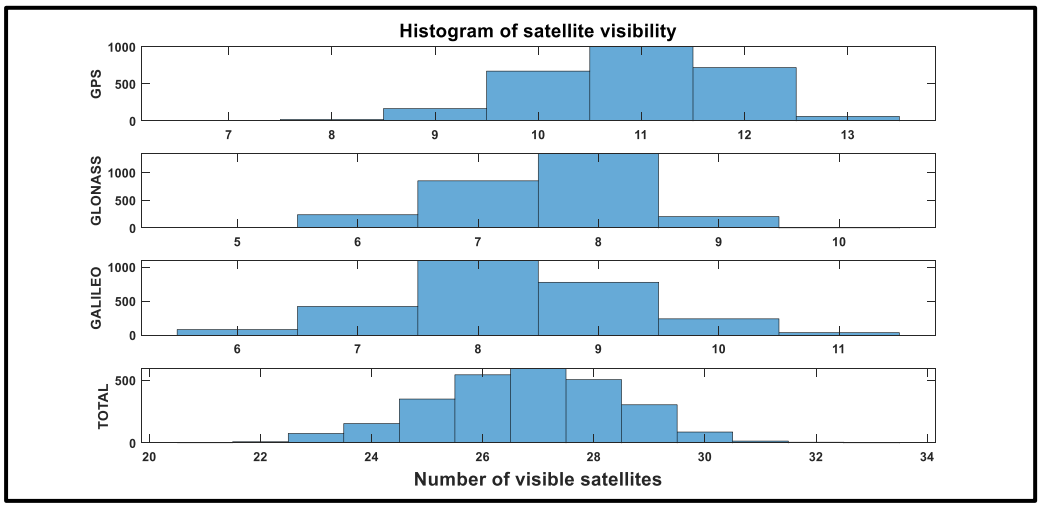

Figure 2. GNSS satellite visibility.

One-second sampled observation data from the excavator and IGS broadcasted navigation data were together used to calculate dilution of precision values and these are plotted along with the number of visible satellites in Figure 3. As can be seen from Figure 2, except a few occasions, the DOP value remains below 2.5.

Signal strength indicators (SSI) obtained from 1 s sampled RINEX 3 data files have been used here as a measure to understand the shadowing environment around the GNSS antenna mounted on the excavator. Figure 4 show plots of the SSI measurements on different frequencies and channels for GPS satellite G04 during the stationary period.

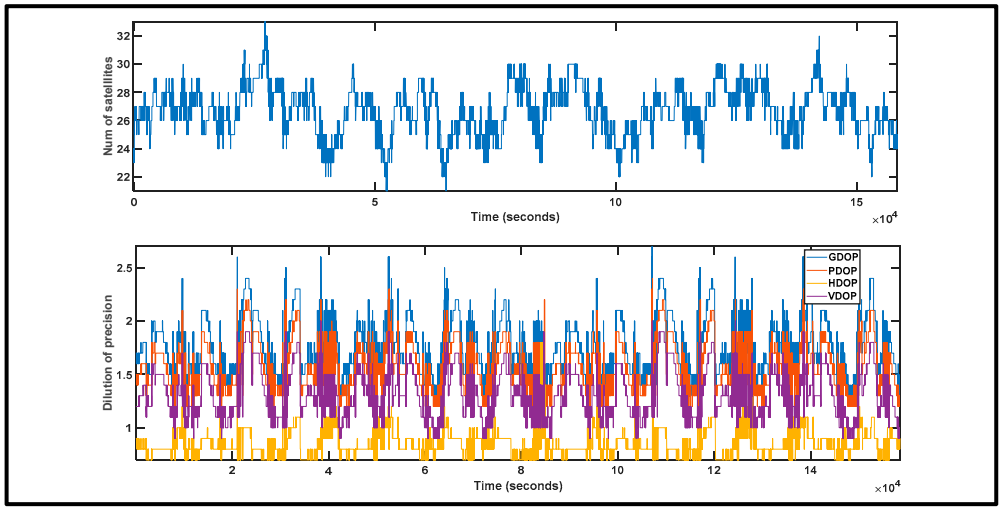

Figure 3. Plot of number of visible satellites and different dilutions of precision (GDOP, PDOP, HDOP and VDOP) as seen at the receiver on the excavator.

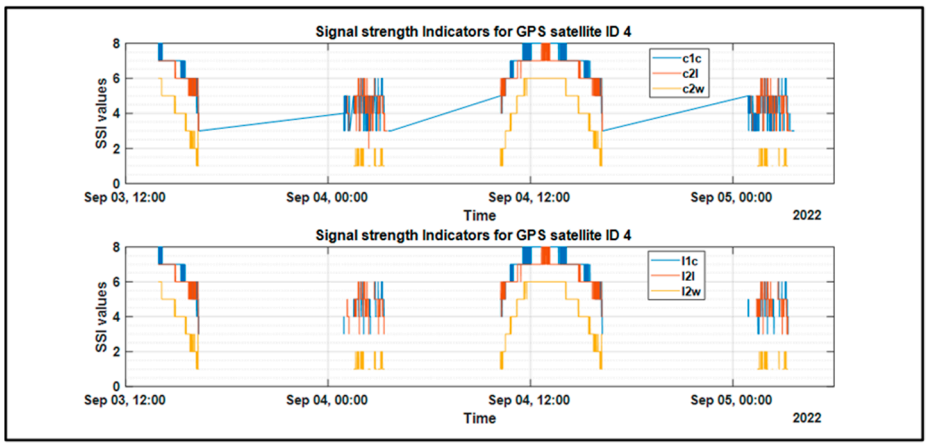

Figure 4. SSI for GPS satellite G04 during the stationary period (3–5 September 2022).

From Figure 4, it appears that C2W and L2W, which are the traditional GPS L2 signals, are weaker in strength than the L2C and L1 C/A signals. SSI values typically range between one and six, which means that the SNR for these signals range between a high of 36–41 dBHz to as low as less than 12 dBHz. Further analysis shows that this weakness of traditional L2 signals is found to be consistent for signals received from all of the GPS satellites. For some satellites, the SSI values for these signals have a maximum of eight or nine. But such cases are few and the time duration for such good signal strength is also very limited. Also from Figure 4, both C2W and L2W seem to be unavailable during certain periods between 2:00 and 3:00 h on 4 September and this is repeated also on 5 September. Also, the pseudorange signals on C1C and C2L seem to be less affected. The anomaly in the SSI measurements of G04 can be further confirmed with a skyplot showing the visibility of the satellites to the excavator antenna during 2:00–3:00 h on 4 and 5 September, and such a skyplot is shown in Figure 5.

As can be seen, the satellite is visible in the NW direction of the excavator during a certain period of time. It is possible that an obstruction (such as a tree) located in this direction blocks the line of sight from the satellite to the receiver antenna causing the drop in signal strength visible in Figure 4.

Figure 6 shows the plot of the SSI for the pseudorange measurements from G04 over varying azimuthal angles around the receiving antenna (during the stationary period).

One can notice anomalous C2W values already at 305° and a total loss of signal strength between 313 and 320° and again between 322 and 329°.

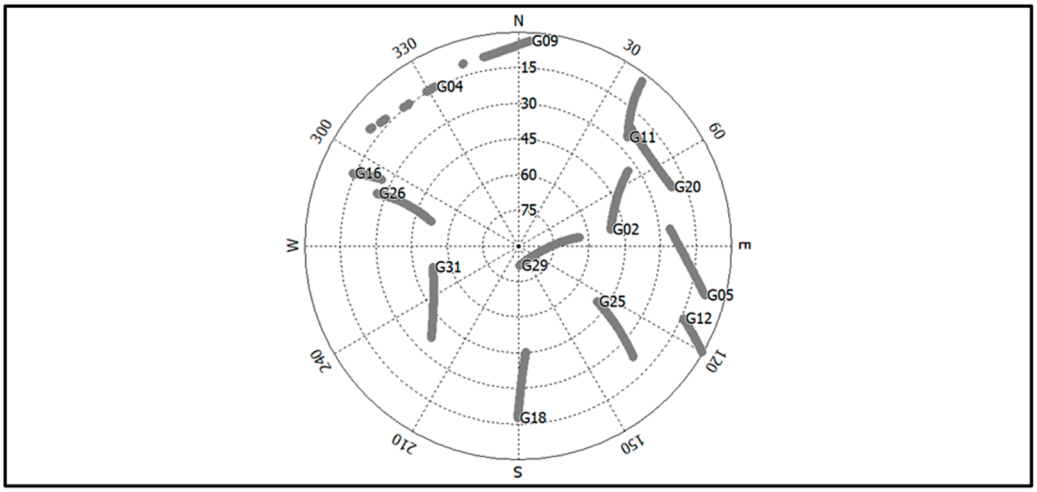

Figure 5. Skyplot showing the visibility of the satellites during 2:00–3:00 h on 4th and 5th September 2022. (The satellite numbers G02, G04 etc. in this case mean the GPS satellite numbers. The numbers on the skyplot indicate increasing values of azimuth in the clockwise direction and increasing values of elevation inwards in the plot).

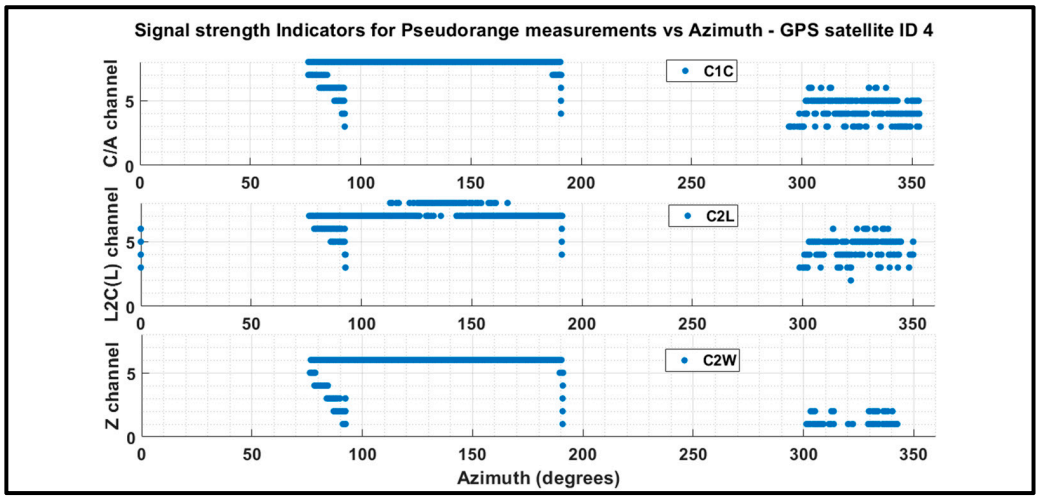

Figure 6. Plot of SSI for code measurements vs azimuth for GPS satellite G04 (during the stationary period).

Similar patterns of signal degradation at these azimuthal angles (around 300–350°) can be noticed for other GPS satellite signals such as those of G07, G09, G10, G14, G18, G23 and G29, as is clear from Figure 7a. Figure 7b clearly shows that C2L performance is much better than C2W.

In order to understand the effect of the obstruction on satellites/signals from other constellations, skyplots of signal strength indicators for C1C and C7Q signals of Galileo satellites E04, E07, E08, E11, E13, E15, E21, E24, E31, E34 and E36 are plotted, as shown in Figure 8 below.

The Galileo signals appear to be quite robust, and although the signal strength is lower at the azimuthal range between 300 and 330°, the signals are received throughout the period.

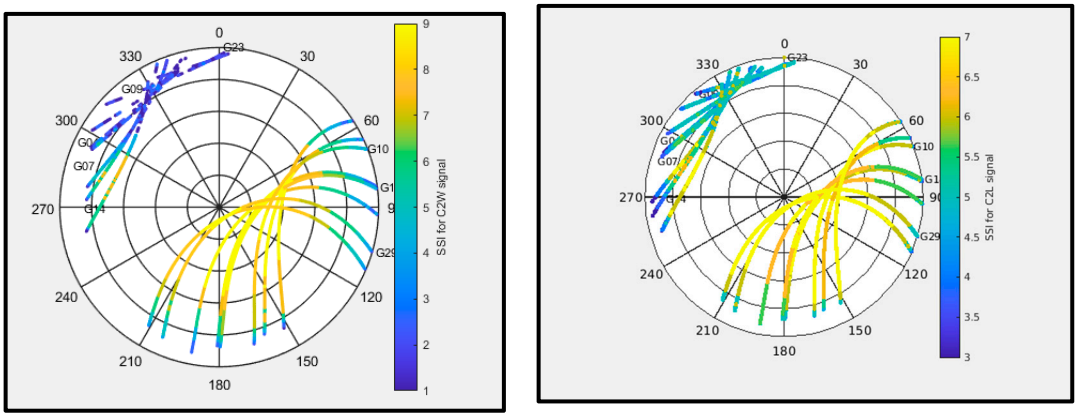

(**a**) (**b**)

Figure 7. Skyplots for different code signals of all affected GPS satellites (G04, G07, G09, G10, G14, G18, G23 and G29) during the stationary period: (**a**) C2W and (**b**) C2L.

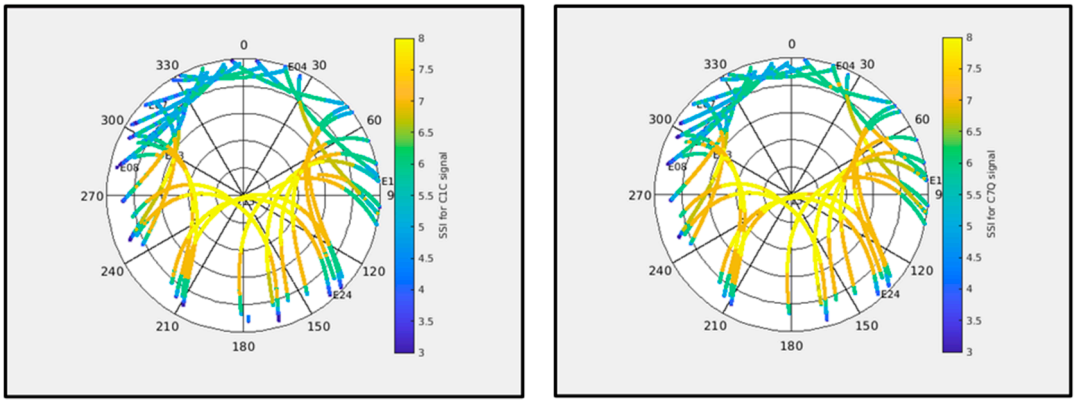

(**a**) (**b**)

Figure 8. Skyplots for different code signals of Galileo satellites during the stationary period: (**a**) C1C and (**b**) C7Q.

4.2. Signal Degradation Due to Reflective Environment

Data collected from the GNSS receiver on the excavator was post processed using GipsyX software version 2.3 to generate pseudorange residuals of the code signal using the Ionosphere-free combination of dual frequency GNSS during the stationary period.

Figure 9 shows the post processed code residuals for GPS using the traditional and the modern GPS signals. One can easily notice the improvement in the performance using the modern L2C GPS signal.

Due to reflective environments, GNSS signals become degraded due to multi-path. But signal degradation is also possible over sharp metallic edges such as that of the roof of the house to the left of the excavator shown in Figure 1c. In such cases, the GNSS signal diffracts or bends over the edge, thus traversing a longer path length than the direct line-of-sight path length and degrading the position computation of the receiver. Thus, the GNSS signal becomes available even in shadowed and non-line-of-sight regions. In order to demonstrate such an effect of signal bending due to reflective environments in the near vicinity of the antenna, controlled experiments were carried out both using the Leica AS10 and high-grade geodetic antenna, as shown in Figure 10a,b.

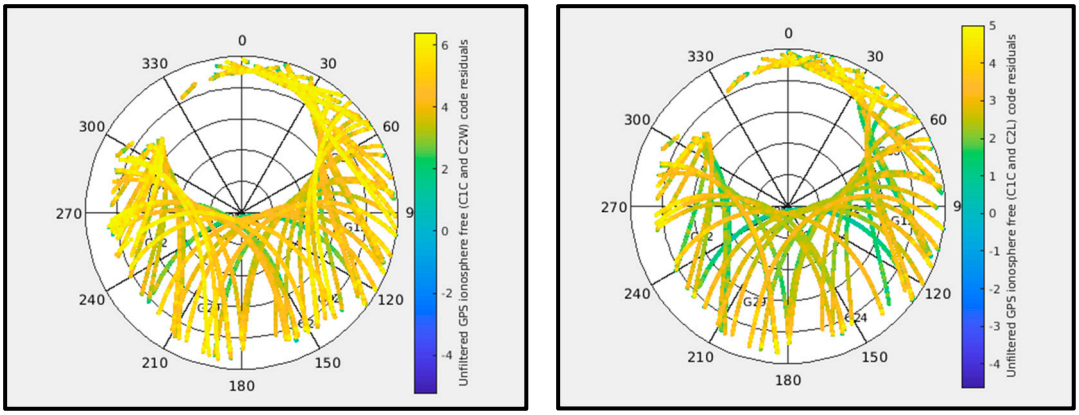

(**a**) (**b**)

Figure 9. GipsyX code residuals using the Ionosphere-free combination of dual frequency GPS. (**a**) Using C1C and C2W; (**b**) using C1C and C2L.

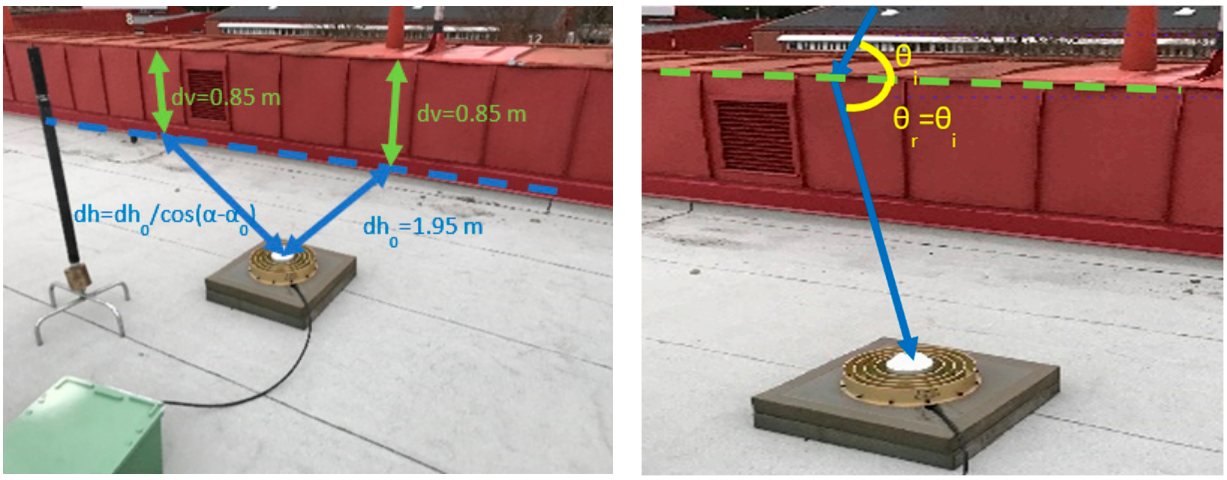

(**a**) (**b**)

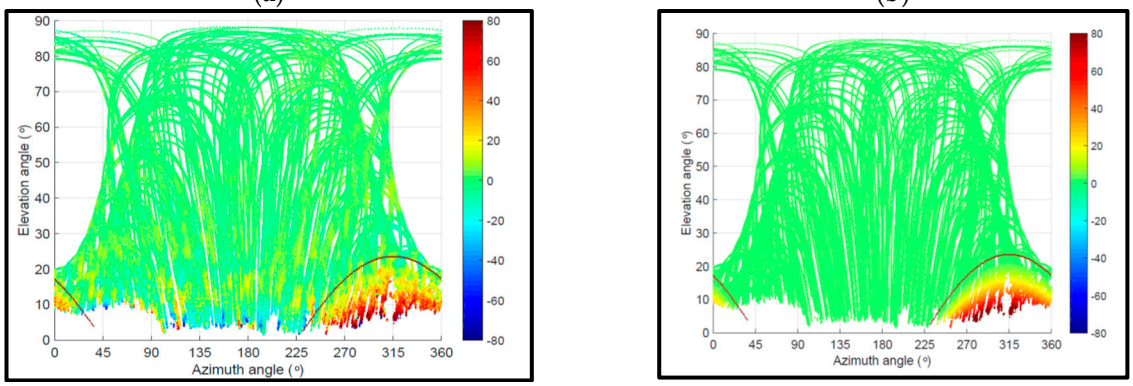

(**c**) (**d**)

Figure 10. *Cont.*

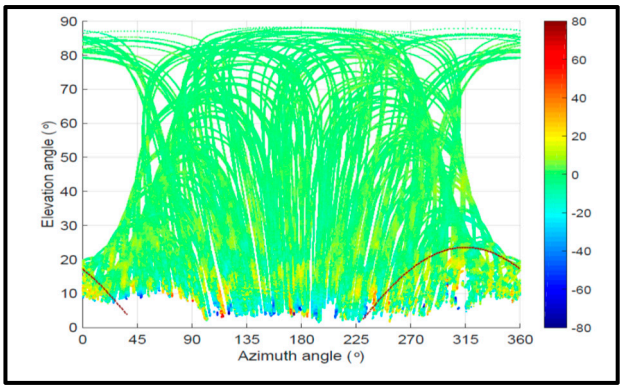

(**e**)

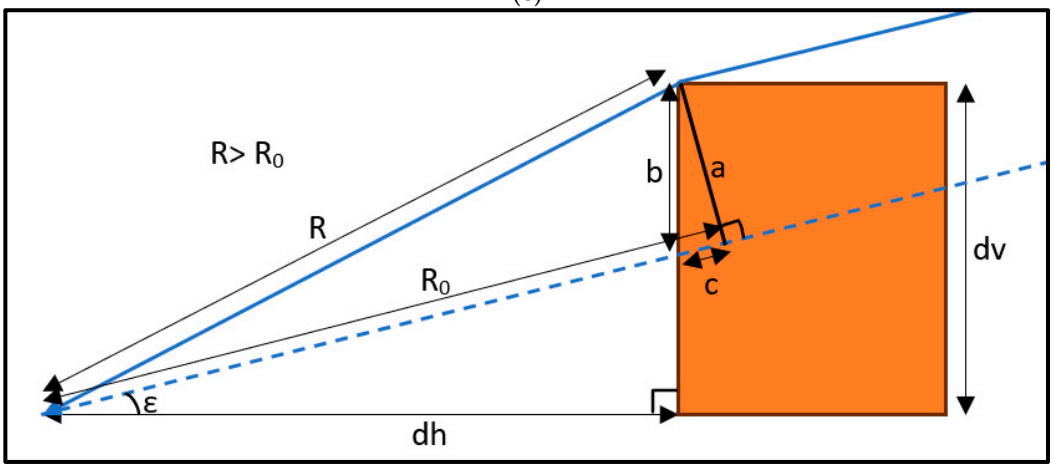

(**f**)

Figure 10. Demonstration of signal degradation due to reflective environments. (**a**) Antenna environment. (**b**) Signal diffraction over metallic edges. (**c**) GPS/GLONASS/Galileo L1/E1 and L2/E5a range residual plots. (**d**) Estimations using a diffraction model. (**e**) Corrected measurements using the model. (**f**) Signal diffraction model (plot dynamics ± 20 mm).

Figure 10c shows a plot of the pseudorange residuals using dual frequency GNSS measurements. The colour bars in Figure 10c–e indicate values of these residuals in mm. The enhanced values of residuals noted at low elevations and an azimuth of 225° to 360° is the effect of signal degradation due to bending over a steel edge, marked with the green dashed line in Figure 10b. The signal diffraction model of Figure 10f is used to estimate the residuals. From Figure 10f, the vertical height of the obstruction is dv and the horizontal distance to the obstruction from the receiver antenna is dh. Thus, for any elevation angle ε, at a given azimuth angle, the path length difference (R–R_0) can be estimated using the following equations.

$$b = dv - dh \cdot \tan(\varepsilon) \tag{1}$$

$$R = \sqrt{\left(dv^2 + dh^2\right)} \tag{2}$$

$$R_0 = \sqrt{\left((dh \cdot \tan(\varepsilon))^2 + dh^2\right)} + c \quad where \quad c = b \cdot \sin(\varepsilon) \tag{3}$$

Variations in dh for varying azimuth angle α can be computed as shown in Figure 10a. A plot of the modelled residuals based on these estimations is shown in Figure 10d. Figure 10e is the plot of the corrected residuals. GNSS signals can also be degraded due to metallic surfaces causing reflections. Such effects are expected to degrade the GNSS signal received on the antenna over the excavator, resulting in erroneous positioning performance.

The signal bending effect as well as signal degradation due to reflective environments will be studied as future work to this paper.

5. Conclusions

Skyplots obtained during the stationary period show that satellites in the NW direction of the excavator during a certain period of time face signal degradation due to a possible obstruction from a tree. Plots of SSI for the carrier phase and code measurements, respectively, from various GPS satellites over varying azimuthal angles around the receiver antenna show anomalous C2W (and L2W) values at around 300–330°. It can be therefore concluded that measurements using C2W (and L2W) may not prove to be very reliable and should be avoided. A similar analysis was conducted, and conclusions were drawn for signals from Galileo. It can also be concluded that Galileo signals are quite robust and reliable and suffer less due to degradation from foliage environments. GNSS signal degradation is also possible due to reflections and bending over sharp metallic edges. As future work, possible reflections from reflective surfaces will be inspected and analysed.

Author Contributions: The document is part of an industrial PhD and is based on the work carried out by U.D. under the supervision of J.J. All authors have read and agreed to the published version of the manuscript.

Funding: This research was funded by Trafikverket and the SiL project grant number TRV 2018/111087, 2019).

Institutional Review Board Statement: Not applicable.

Informed Consent Statement: Not applicable.

Data Availability Statement: The data presented in this study are available upon request from the authors.

Acknowledgments: The authors acknowledge NASA and Jet Propulsion Laboratory for the GipsyX Precise Point Positioning software package.

Conflicts of Interest: The authors declare no conflict of interest.

References

1. Dutta, U.; Jarlemark, P.; Rieck, C.; Johansson, J. Ionospheric Effects on GNSS RTK. In Proceedings of the 35th International Technical Meeting of the Satellite Division of The Institute of Navigation (ION GNSS+ 2022), Denver, CO, USA, 19–23 September 2022; pp. 1589–1598. [CrossRef]
2. McCaffrey, A.M.; Jayachandran, P.T.; Langley, R.B.; Sleewaegen, J.M. On the accuracy of the GPS L2 observable for ionospheric monitoring. *GPS Solut.* **2017**, *22*, 23. [CrossRef]
3. Andrei, C.-O.; Lahtinen, S.; Poutanen, M.; Koivula, H.; Johansson, J. Galileo L10 Satellites: Orbit, Clock and Signal-in-Space Performance Analysis. *Sensors* **2021**, *21*, 1695. [CrossRef] [PubMed]
4. Andrei, C.O.; Johansson, J.; Koivula, H.; Poutanen, M. Signal performance analysis of the latest quartet of Galileo satellites during the first operational year. In Proceedings of the 2020 International Conference on Localization and GNSS (ICL-GNSS), Tampere, Finland, 2–4 June 2020; pp. 1–6.
5. Montenbruck, O.; Steigenberger, P.; Hauschild, A. Comparing the 'Big 4'—A User's View on GNSS Performance. In Proceedings of the 2020 IEEE/ION Position, Location and Navigation Symposium (PLANS), Portland, OR, USA, 20–23 April 2020; pp. 407–418.
6. Bertiger, W.; Bar-Sever, Y.E.; Dorsey, A.; Haines, B.; Harvey, N.; Hemberger, D.; Heflin, M.; Lu, W.; Miller, M.; Moore, A.W.; et al. GipsyX/RTGx, a new tool set for space geodetic operations and research. *Adv. Space Res.* **2020**, *in press*. [CrossRef]
7. Zumberge, J.F.; Heflin, M.B.; Jefferson, D.C.; Watkins, M.M.; Webb, F.H. Precise point positioning for the efficient and robust analysis of GPS data from large networks. *J. Geophys. Res.* **1997**, *102*, 5005–5017. [CrossRef]

Disclaimer/Publisher's Note: The statements, opinions and data contained in all publications are solely those of the individual author(s) and contributor(s) and not of MDPI and/or the editor(s). MDPI and/or the editor(s) disclaim responsibility for any injury to people or property resulting from any ideas, methods, instructions or products referred to in the content.